Thermoplastic Elastomers Based on Strong and Well-Defined Hydrogen-Bonding Interactions

Serge H. M. Söntjens,[†] Raymond A. E. Renken,[‡] Gaby M. L. van Gemert,[‡] Tom A. P. Engels,[§] Anton W. Bosman,[⊥] Henk M. Janssen,[‡] Leon E. Govaert,[§] and Frank P. T. Baaijens*[,†]

Soft Tissue Biomechanics and Engineering, Biomedical Engineering, Eindhoven University of Technology, PO Box 513, 5600 MB Eindhoven, The Netherlands; SyMO-Chem BV, PO Box 513, 5600 MB Eindhoven, The Netherlands; Polymer Technology, Mechanical Engineering, Eindhoven University of Technology, PO Box 513, 5600 MB Eindhoven, The Netherlands; and SupraPolix BV, Horsten 1, 5612 AX Eindhoven, The Netherlands

Received April 3, 2008; Revised Manuscript Received June 3, 2008

ABSTRACT: In order to investigate the effects of strong and well-defined hydrogen bonding on the properties of thermoplastic elastomers (TPEs), we have applied two distinct and strongly dimerizing 2-ureido-4-[1*H*]-pyrimidinone (UPy) quadruple hydrogen-bonding units as physical cross-linker. While the UPy groups consequently serve as the "hard phase" or "hard block" in these TPEs, an amorphous polyester has been used as the "soft phase" or "soft block". The UPy unit has been flanked with either a sterically demanding isophorone spacer or a linear hexamethylene, where these spacers have been derived from isophorone diisocyanate (IPDI) or hexamethylene diisocyanate (HDI), respectively. This difference on a molecular level leads to a homogeneous amorphous material in the IPDI case (polymer **1**) and to a nanophase-separated material in the HDI case (polymer **2**) as revealed by AFM and DSC experiments. Apart from this distinctive difference in morphology and nanoscopic organization, the macroscopic properties of both materials are also fundamentally different. In linear stress−strain and DMTA experiments, the homogeneous IPDI material **1** shows rubberlike behavior at room temperature, while the mechanical properties are strongly temperature dependent. The nanophase-separated HDI material **2** shows a combination of rubber and plastic behavior and displays a clear rubber plateau between 0 and 50 °C with little temperature dependence. The apparent activation energy of flow for the latter material, determined by multifrequency DMTA, is 135 kJ mol^{-1}.

Introduction

In the field of synthetic macromolecules,[1] thermoplastic elastomers[2] (TPEs) are a valuable addition to the classical division between thermoplastic and thermosetting polymers, the latter including vulcanized rubbers. TPEs combine the ease of processing of a thermoplastic material with the favorable mechanical properties of a rubber. These specific properties are a result of the morphology of the material. Usually, a TPE material is a segmented block copolymer that contains (1) an amorphous or semicrystalline polymer block with a low-temperature glass transition and (2) a block that physically cross-links the polymer chains into a reversible network. The amorphous or semicrystalline polymer, which is commonly referred to as the "soft phase" or the "soft block", is microphase-separated from the cross-linking "hard phase" or "hard block", which consists of e.g. a nonmiscible crystalline copolymer[2,3] or a hydrogen-bonding[4] urethane[5,6] or urea segment.[7,8] The reversibility of the cross-links in TPEs leads to fundamental differences in mechanical properties between these materials and rubbers. Whereas chemically and irreversibly cross-linked rubbers show fully elastic deformation, the physically and reversibly cross-linked thermoplastic elastomers display a combination of plastic and elastic deformation behavior. Plastic deformation, however, can only occur when the reversible cross-links are disrupted by thermal or mechanical means. As a result, it is possible to enhance the elastic nature of TPE materials by strengthening the reversible cross-links.

Thermoplastic elastomers that are physically cross-linked by hydrogen-bonding interactions most commonly employ urethane and urea groups, with respective free energies of association in the order of 0−4[9] and 17−22[10] kJ mol^{-1} in an apolar environment (CCl_4). These binding energies are moderate compared to many well-defined molecular systems that have been developed in the field of supramolecular chemistry.[11,12] The 2-ureido-[1*H*]-pyrimidin-4-one or UPy[13–15] moiety, for example, shows a self-complementary dimerization that involves four hydrogen bonds where the dimerization free energy is in the order of 44−50 kJ mol^{-1} at room temperature in organic solvents such as $CDCl_3$ or toluene.[15] See Scheme 1 for the molecular structure of the UPy dimer. We have investigated the influence of such strong hydrogen-bonding interactions of the UPy moiety on the morphology and mechanical properties of TPE.

The quadruple hydrogen-bonding UPy unit has been coupled to polymer chains previously, where the focus was on modifica-

Scheme 1. Molecular Structure of the 2-Ureido-[1*H*]-pyrimidin-4-one (or UPy) Dimer, Displaying Four Intermolecular Hydrogen Bonds and One Intramolecular Hydrogen Bond[a]

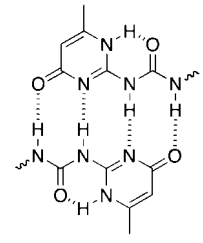

[a] The dashed lines indicate the hydrogen bonds.

* Corresponding author. E-mail: f.p.t.baaijens@tue.nl.
[†] Biomedical Engineering, Eindhoven University of Technology.
[‡] SyMO-Chem BV.
[§] Mechanical Engineering, Eindhoven University of Technology.
[⊥] SupraPolix BV.

10.1021/ma800744c CCC: $40.75
Published on Web 07/11/2008

Scheme 2. Synthesis of TPE Polymers 1 and 2 from Telechelic Hydroxy-Terminated Poly(2-methyl-1,3-propylene adipate) with a Molecular Weight of 2 kg mol^{-1} and the Bifunctional IPDI-UPy-IPDI or HDI-UPy-HDI Isocyanate Synthons[a]

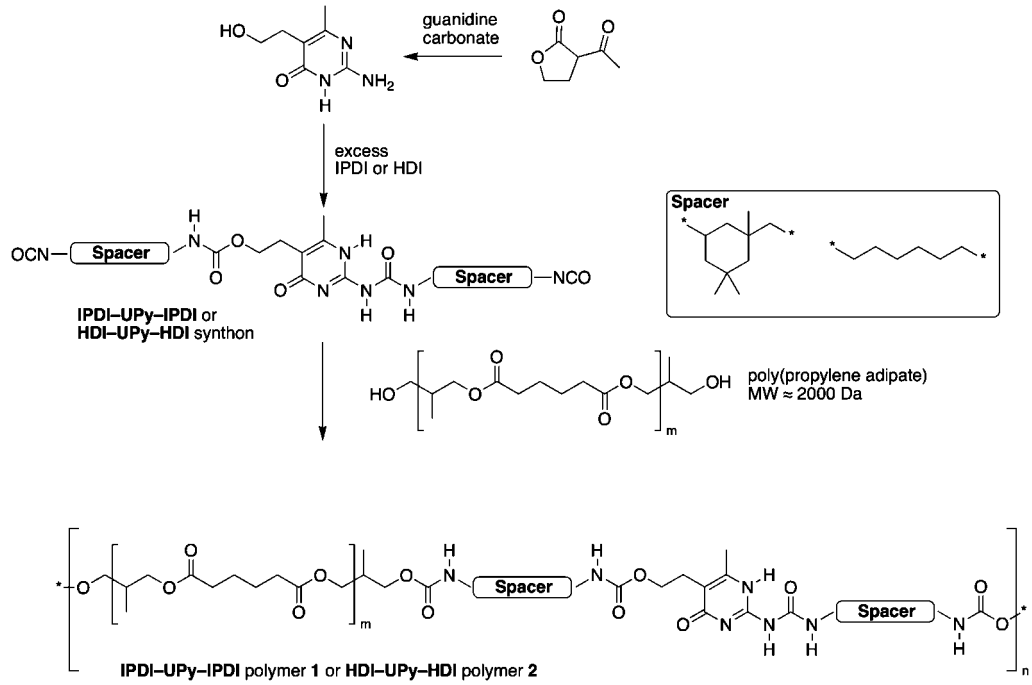

[a] The chosen average number of UPy units in the polymer backbone is $n = 6$.

tion of telechelic macromolecules of various origins, e.g., polyesters, polycarbonates, polyethers, or poly(ethylene butylenes).[14,16–18] Polyacrylates or polymethacrylates with pending UPy units have also been synthesized and investigated.[19–22]

In this work, we report the strongly interacting UPy moiety as the hard block in segmented copolymeric TPEs, employing an amorphous polyester, specifically a polyadipate with a molecular weight of 2 kg mol^{-1}, as the soft block. We have connected the UPy moiety to the polyester main chain by using two different linkers. One linker was derived from the sterically demanding and geometrically irregular isophorone diisocyanate (IPDI) molecule and the other from the linear and regular hexamethylene diisocyanate (HDI) molecule. The prepared materials have been characterized by using various techniques such as DSC, AFM, tensile testing, and DMTA in order to investigate the nature of and the differences between the prepared TPEs. Specifically, we were interested in the morphology of the materials and how this morphology would affect mechanical properties.

Experimental Details

Synthesis. All synthetic procedures as well as the details on the analytical methods used to characterize the prepared building blocks and polymer materials are gathered in the Supporting Information.

Differential Scanning Calorimetry (DSC). DSC was performed on a Mettler-Toledo DSC823 DSC instrument. The DSC was also equipped with a SO801RO sample robot and a Lauda RC25 CS cryostat. Mettler-Toledo aluminum sample pans with a volume of 40 μL were used for all experiments. The samples for the annealing experiments (performed in duplo) were cycled from 25 to 100 °C until no more changes were observed in the thermogram. The samples were then allowed to anneal at a set temperature for a predetermined time. The melting peak in the first heating run was subsequently analyzed.

Atomic Force Microscopy (AFM). AFM micrographs were recorded at 37 °C in air on cast films of the materials, using a Digital Instruments Multimode Nanoscope IV, operating in the tapping regime mode with silicon cantilever tips (PPP-NCH-50, 204−497 kHz, 10−130 N m^{-1}) with scan rates between 0.5 and 1.0 Hz. All micrographs were subjected to a first-order plane-fitting procedure to compensate for sample tilt.

Tensile Testing. Tensile testing was performed on a Zwick (Ulm, Germany) Z-010 tensile testing instrument, using an AST (Angewandte System-Technik GmbH, Dresden, Germany) 2.5 kN KAF-Z force transducer at room temperature. Uniaxial stress−strain experiments were performed according to ASTM D 1708-96, on dog-bone-shaped tensile test bars that had been punched from films of material. Experiments were conducted at room temperature, with a crosshead speed of 0.3 mm s^{-1}, resulting in a strain rate of ≈1.3 $\times$ 10^{-2} s^{-1}. Representative results were obtained by producing and testing $n = 5$ specimens.

Dynamic Mechanical Thermal Analysis (DMTA). DMTA was performed on films of the polymers, with a TA Instruments (New Castle, DE) Q800 dynamic mechanical thermal analyzer (DMTA) at a maximum strain of 0.1% and a heating rate of 0.5 K/min with a TA Instruments film tension clamp that was recalibrated before every experiment. To obtain optimal clamping conditions, all samples were cooled below their glass transition temperature (∼−70 °C) before clamping. The experiments at multiple frequencies were performed on one sample (in duplo) in isothermal steps of 2 °C. The position of the alpha transition in the HDI material was determined from the peak in the loss modulus E'' by fitting a linear baseline and a Gaussian peak function to the data.

Results

Synthesis.[23,24] In Scheme 2, the route is shown that is used to prepare the thermoplastic elastomers **1** and **2**. The commercially available 2-acetyl butyrolactone is condensed with guanidine carbonate to produce 5-hydroxyethyl-6-methylisocytosine. This bifunctional isocytosine is reacted with an excess of isophorone diisocyanate (IPDI) or hexamethylene diisocyanate (HDI), rendering the IPDI-UPy-IPDI and the HDI-UPy-HDI synthons. Note that the HDI-derived synthon is a single product and that the IPDI-derived synthon is in fact a mixture of 16 isomers because IPDI is a mixture of cis and trans isomers and because the primary and secondary isocyanates of IPDI can both react in the applied reaction condtions.[25] Finally, the UPy

diisocyanate building blocks have been used to chain extend the telechelic and amorphous poly(2-methyl-1,3-propylene adipate), where the molar ratio between both reactants can be chosen to determine the molecular weight of the polymer product and the average number of UPy units in the polymer backbone.

The two chain-extended polyesters **1** and **2** have comparable molecular weights ($M_n \sim 15$ kDa, as determined by SEC), and this result is in line with the chosen average number of UPy units per polymer chain ($n = 6$). Chain extension to $n = 6$ has been selected after a study where the number of UPy units were systematically increased from 3 to about 30−40, using the IPDI-UPy-IPDI synthon. It was found that polymers with on average six UPy units in the polymer backbone already show much improved mechanical properties, while still being of relatively low molecular weight, enhancing their processability. See the Supporting Information for details on this study.

Thermal Properties. Differential scanning calorimetry (DSC) has been used to assess the thermal properties of the IPDI- and HDI-based UPy polymers **1** and **2**. A glass transition was found at −38 °C for the IPDI polymer 1 and at −46 °C for the HDI polymer 2. The glass transition of the HDI polymer is significantly closer to that of the propylene adipate prepolymer at −57 °C, indicating more pronounced phase separation in the latter material. The IPDI polymer **1** shows no visible transitions between 25 and 100 °C, which is typical for a homogeneous, amorphous system. The HDI polymer **2**, however, displays a clear melting transition in the first heating run at 78 °C, reinforcing the notion of strong phase separation in this material. Representative DSC traces are included in the Supporting Information.

The formation of the crystalline phase in the HDI polymer **2** has been further investigated by isothermal crystallization experiments. Results from the first heating run usually cannot be interpreted reliably, as these are strongly influenced by the (thermal) history of the sample and by the contact of the sample with the bottom of the DSC pan. In order to delete the (thermal) history, samples are first heated cyclically from room temperature to 100 °C until no more changes are observed in the DSC trace. Samples are then allowed to crystallize at a chosen temperature and for a chosen period of time. In a subsequent DSC experiment the melt transition in the first heating run was analyzed (see Figure 1 for results). It is evident that both the peak melting temperature and the enthalpy of fusion shift as a function of crystallization time and the extent of supercooling.

On one hand (Figure 1a), higher annealing temperatures lead to higher melting transition temperatures. For example, allowing the sample to crystallize at 50 °C for a few hours results in a higher melting temperature than annealing for weeks at room temperature. The changes in peak melting temperature are presumably due to either (1) a change in the size of the crystals formed or (2) a change in crystal-defect fraction. Remarkably, it is evident in Figure 1b that annealing at temperatures closer to the melting transition seems to lower the enthalpies of fusion, although this is only pronounced for samples annealed at 50 °C.

We can reasonably assume that the enthalpy of fusion is linearly related to the (volume) fraction of the crystalline phase. The enthalpy data have thus been evaluated with a modified Avrami[26] equation:

$$\Delta H_m = \Delta H_{m,\infty}(1 - e^{-kt^n}) \quad (1)$$

where the exponent n indicates the order of crystallization, with $n = 1$ for linear or one-dimensional crystallization, $n = 2$ for platelike or two-dimensional crystallization, and $n \geq 3$ for three-dimensional crystallization. The crystallization order parameters n, determined from the fits to the Avrami equation in Figure 1b, are 0.83 ± 0.06 (30 °C), 0.73 ± 0.10 (40 °C), and 0.74 ± 0.13 (50 °C). These results support one-dimensional crystallization, presumably stacks of dimerized UPy moieties, although the values found for the order parameter are even lower than the expected $n = 1$.

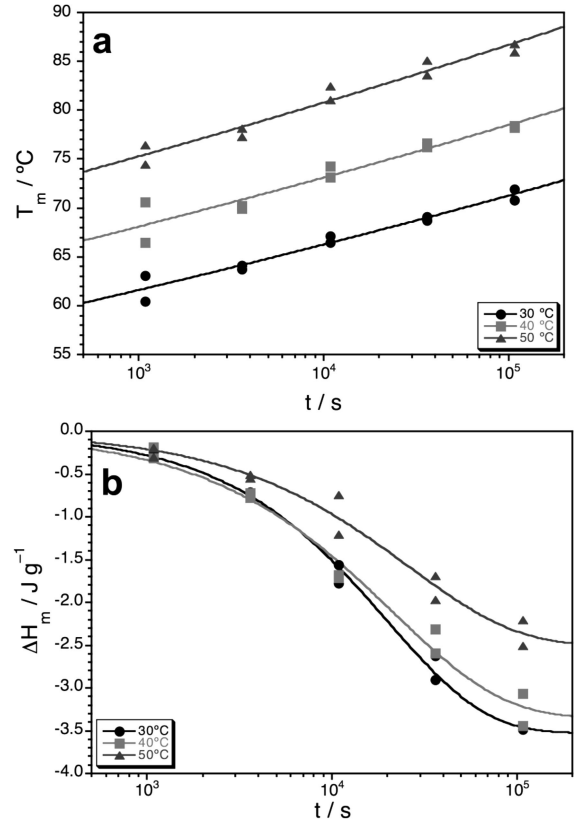

Figure 1. Crystallization experiments on HDI polymer **2**. (a) Peak melting temperature as a function of annealing time at an annealing temperature of 30, 40, or 50 °C. The solid line serves to guide the eye. (b) Enthalpy of fusion as a function of crystallization time at 30, 40, or 50 °C. The solid line represents a fit to the modified Avrami equation.

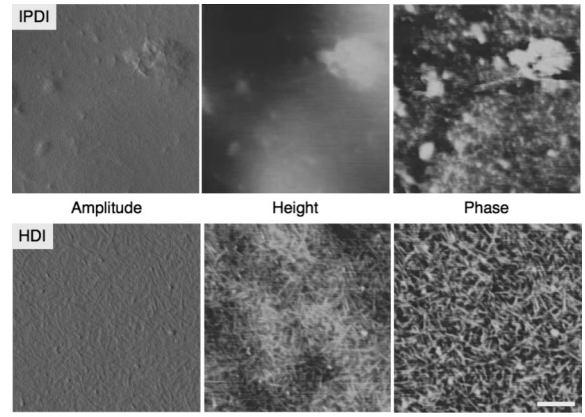

Figure 2. Atomic force micrographs of the IPDI and HDI materials **1** and **2**, showing no evidence for a nanostructure in the case of the IPDI material, and a wormlike hard-block structure in a soft matrix for the HDI material (the bar represents 100 nm).

Atomic Force Microscopy. Tapping mode AFM[27] is an excellent technique to examine thermoplastic elastomers because differences between hard and soft blocks can easily be distinguished in AFM phase data. AFM micrographs of cast films of the HDI material **2** depicted in Figure 2 show wormlike hard structures in a soft matrix. The worm structures are about 100

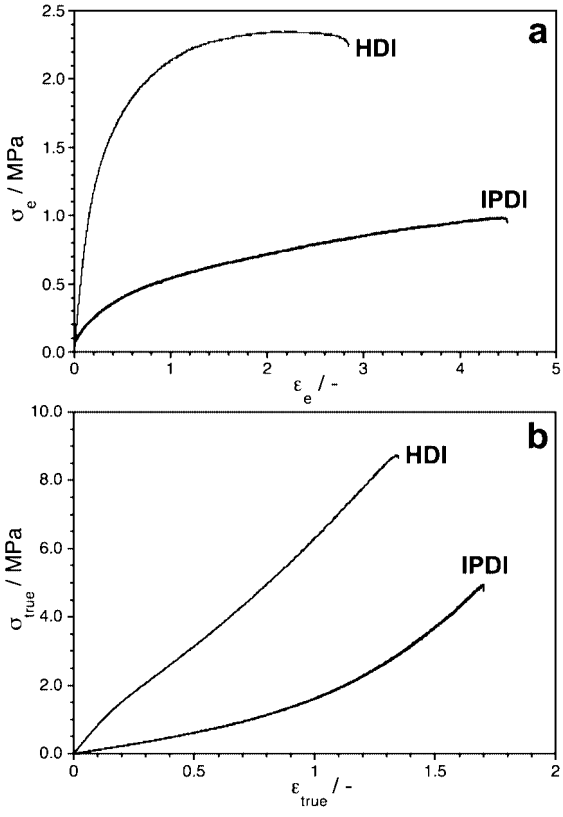

Figure 3. Representative one-dimensional stress−strain experiments performed on dog-bone-shaped tensile test bars of the IDPI and HDI materials **1** and **2** (room temperature, crosshead speed of 300 μm s^{-1}), showing (a) the engineering stress and strain and (b) the true stress and strain, calculated as $\varepsilon_{true} = \ln(1 + \varepsilon_e)$ and $\sigma_{true}=(1 + \varepsilon_e)\sigma_e$.

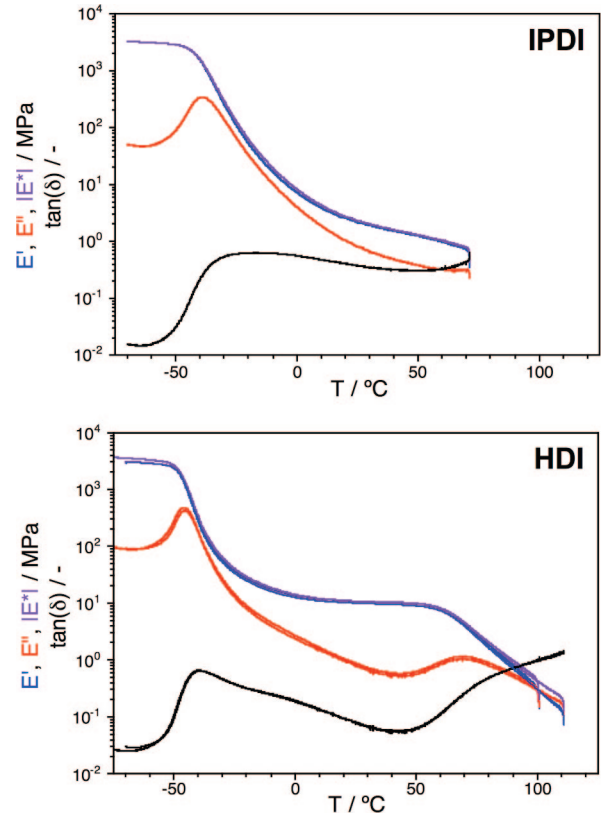

Figure 4. DMTA traces (duplo, 1 Hz, 0.1% deformation) of the IPDI and HDI polymers **1** and **2**, showing the storage modulus E', the loss modulus E'', the complex modulus $|E^*|$, and the tan(δ). The IPDI polymer shows a gradual drop in modulus beyond the glass transition, whereas the HDI polymer shows a clear rubber plateau region (0 to about 50 °C).

nm in length and are smaller than 10 nm in width; we interpret them as one-dimensional crystalline stacks of dimerized UPy moieties. No organized (nano)structure is visible in the AFM data of the IPDI material **1**.

The AFM micrographs support the evidence shown by DSC that the HDI material **2** contains a phase-separated crystalline phase and that the IPDI material **1** is fully amorphous. Furthermore, the observed crystalline structures in material **2** are most likely one-dimensional crystals of dimerized UPy units, which is in line with the interpretation of the isothermal crystallization experiments using the Avrami equation.

Stress−Strain Experiments. Uniaxial stress−strain experiments have been performed on dog-bone-shaped tensile bars punched from cast films of materials **1** and **2**, showing marked differences between the recorded stress−strain curves of both materials. First, the Young's modulus of the HDI material is significantly higher at 7.7 ± 0.3 MPa, compared to only 1.2 ± 0.1 MPa for the IPDI material. This is presumably due to the additional cross-linking provided by the nanophase-separated crystals present in the HDI material.

Second, the overall shape of the engineering stress−strain curves in Figure 3a also indicates differences between the two materials. The IPDI material shows classical rubberlike behavior, with two relatively linear regimes at low and high deformation, and no evidence of a yieldlike component. The ultimate tensile strength ($\sigma_T = 0.97 \pm 0.04$ MPa) is reached at maximum strain ($\varepsilon_{max} = 4.4 \pm 0.2$) and failure is sudden. The HDI material, in contrast, shows a combination of rubber- and yieldlike behavior. The ultimate tensile strength ($\sigma_T = 2.40 \pm 0.04$ MPa) is reached before the maximum strain is ($\varepsilon_{max} = 3.1 \pm 0.2$), and a subsequent decrease in stress is observed until failure.

The shape of the true stress vs true strain curves in Figure 3b supports the elastic nature of both materials but also shows differences between the two TPEs. Significant strain hardening is evident in both materials, resulting in a clearly visible and significant increase in the slope of the true stress−strain curve in the case of the IPDI material, and a nearly linear curve in the case of the HDI material. The shape of the true stress−strain curve for the IPDI material indicates homogeneous deformation, whereas the shape of the engineering curve for the HDI material indicates inhomogeneous deformation, although no macroscopic inhomogeneous deformation was observed.

Dynamic Mechanical Thermal Analysis. The mechanical properties of the two thermoplastic elastomers **1** and **2** at small deformations have been studied by performing dynamic mechanical thermal analysis (DMTA) on films of both materials. The DMTA thermograms in Figure 4 clearly show that materials **1** and **2** are significantly different at the imposed small deformations. While the materials behave essentially identical at temperatures below the glass transition temperature (T_g), the glass transition itself is both more well-defined and shifted to lower temperature for the HDI material **2**, demonstrating that phase separation is strong in this material and confirming the results that have been obtained in the DSC experiments (vide supra). When temperature is increased beyond the glass transition, the IPDI material **1** shows a gradual decrease in modulus, eventually leading to flow around 70 °C. The HDI material shows more complex behavior as a function of increasing temperature, including a rubber plateau from 0 to about 50 °C, followed by a clear melting transition (T_α), a subsequent gradual decrease in mechanical properties, and eventually flow.

DMTA at Multiple Frequencies. In order to get more insight into the kinetics of the melting transition and the preceding rubber plateau in the HDI polymer **2**, DMTA experiments were

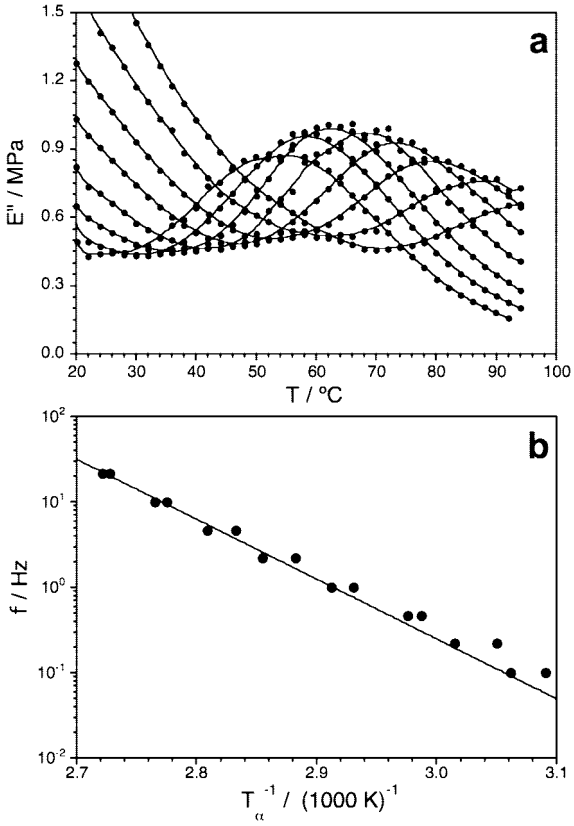

Figure 5. (a) Expansion of the peak in the loss modulus E'' for the HDI material **2**; multiple DMTA thermograms for different frequencies are plotted (0.1, 0.2, 0.5, 1, 2, 5, 10, and 20 Hz; the line serves to guide the eye). Increasing the frequency from 0.1 to 20 Hz leads to a gradual shift in melting temperature T_α to higher temperatures. (b) Arrhenius plot of the temperature T_α as a function of frequency for the HDI material, yielding an apparent activation energy for flow for this transition at 135 ± 6 kJ/mol ($r^2 = 0.993$).

performed with frequencies varying from 0.1 to 20 Hz. The transition temperature T_α was defined here as the maximum in the loss modulus E'' as a function of temperature (Figure 5a) and was modeled as an Arrhenius process (Figure 5b). This evaluation yields an apparent activation energy for flow in the rubber plateau of 135 ± 6 kJ mol^{-1} for this material.

Discussion and Conclusions

We have studied thermoplastic elastomers **1** and **2** that have been prepared from similar building blocks, with both materials having on average six UPy-based physical cross-linkers incorporated in a polyester backbone. The UPy units in polymer **1** are flanked by IPDI-derived spacers, whereas in polymer **2** the UPy units have HDI-derived flanking spacers. Combined data from an AFM and a DSC study show that the IPDI polymer **1** is fully amorphous, while the HDI polymer **2** contains a crystalline fraction consisting of nanoscopic rods. The rods are presumably stacks of dimerized UPy units. Apparently, the regular linear hexamethylene spacer in material **2** allows for crystallization and formation of a distinct nanostructure, presumably with assistance of the distal urethanes in the crystallization process. In contrast, the steric bulk and geometric irregularity of the isophorone spacer in polymer **1** effectively inhibits and frustrates crystallization of UPy units, despite the presence of the distal urethane groups. These results are in line with a previous study on telechelic poly(ethylene−butylene)s bearing two UPy end groups, as also in these systems the formation of well-defined wormlike nanostructures is observed when urethane or particularly urea groups are close to the UPy moiety.[28] Steric constraints in the spacer had not been investigated in this study.

Isothermal crystallization experiments using DSC show that the formation of the crystalline phase in the HDI material **2** is a slow process. This may be due to the slow dissociation kinetics of the UPy moiety, with predissociation lifetimes that can extend into the second regime,[15] leading to a decreased mobility of individual chains. A crystallization order parameter of 0.77 is found for the HDI material by evaluation of the crystallization kinetics using an Avrami model. This number is below the value of unity that is expected for linear or one-dimensional crystallization, but it nonetheless supports linear crystallization compared to two- or three-dimensional crystallization, where much higher values of 2−4 are expected. Additionally, the linear crystallization kinetics are in line with the hard phase nanoscopic rods, presumably one-dimensional crystals of dimerized UPy units, which are observed experimentally using AFM.

The molecular and nanoscopic differences between materials **1** and **2** lead to marked differences in the macroscopic mechanical properties. At low deformation in a one-dimensional stress−strain experiment, both materials are elastic, but at higher deformations the IPDI and the HDI materials react differently. The IPDI material **1** shows stress−strain curves that are reminiscent of classical rubberlike materials, displaying strain hardening and indicating a homogeneous deformation process. The HDI material **2**, however, displays a combination of rubber and plastic properties, showing a much steeper strain response that incorporates a small yield component. Even at low deformations in DMTA experiments, clear differences between the two materials can be observed. In the DMTA experiment, the probed temperature range (−50 to 100 °C) corresponds to a decrease in association constant of the UPy moiety of approximately 4 orders of magnitude. For the IPDI material **1**, this increase in molecular dynamics leads to a gradual decrease in average cross-link density (or increase in cross-link dynamics), which in turn leads to a gradual decrease in mechanical properties. The crystalline nature of the hard block in the HDI material **2** prevents this behavior. Beyond the glass transition the material is cross-linked by stacks of UPy dimers, where these dimers cannot dissociate until these stacks melt. When the stacks eventually start melting around 50 °C, the behavior of the material becomes similar to that of the IPDI material on both nanoscopic and macroscopic scales, including a gradual decrease of mechanical properties with increasing temperature and eventually flow at 100−120 °C.

In this work, we have described two thermoplastic elastomers **1** and **2** which show a rational correlation between molecular configuration, nanoscopic morphological structure, and bulk or macroscopic mechanical properties. These properties can be tuned from classical rubberlike behavior to a more complex combination of elastic and plastic behavior, simply by changing the spacer that connects the cross-linking moiety to the polymer. Also, the variation in the number of UPy units in the polymeric backbone can be used to tailor the properties of these kind of materials (see the Supporting Information for examples).

The advanced elastomers described here may have a variety of applications, in e.g. medical devices, tissue engineering, and nanotechnology. In fact, we have selected the HDI polymer **2** for use as a tissue engineering material in blood vessels, particularly because of its advantageous elastic features (displaying a rubber plateau and a minimum of the tan δ around 37 °C), while still being easily processable from solution, having a molecular weight of only 15 kDa. The UPy groups on the surface and in the bulk of this material also allow it to act as a versatile platform for supramolecular functionalization with UPy-functionalized species, permitting facile surface or bulk modification with e.g. bioactive moieties such as prodrugs or

oligopeptide cell binding domains, an approach that has been explored by Dankers et al.[29–31]

Acknowledgment. Senter/Novem is gratefully acknowledged for providing funding for these investigations. The authors also thank Eva Wisse for the AFM micrographs presented in this manuscript.

Supporting Information Available: Additional materials and methods, DSC traces and synthetic methods of the materials discussed above, and synthesis and analysis of materials with longer and shorter chain length. This material is available free of charge via the Internet at http://pubs.acs.org.

References and Notes

(1) Staudinger, H. *Die Hochmoleculare Organische Verbindungen*; Springer: Berlin, 1932.
(2) Legger, N. R.; Holden, G.; Schroeder, H. E. *Thermoplastic Elastomers: A Comprehensive Review*; Carl Hanser Verlag: Munich, 1987.
(3) Coleman, D. *J. Polym. Sci.* **1954**, *14*, 15–28.
(4) Latimer, W. M.; Rodebush, W. H. *J. Am. Chem. Soc.* **1920**, *42*, 1419–1433.
(5) Bonart, R. *J. Macromol. Sci. B* **1968**, *2*, 115–138.
(6) Bonart, R.; Morbitzer, L.; Hentze, G. *J. Macromol. Sci. B* **1969**, *3*, 337–356.
(7) Bonart, R.; Morbitzer, L.; Muller, E. H. *J. Macromol. Sci. B* **1974**, *9*, 447–461.
(8) Versteegen, R. M.; Sijbesma, R. P.; Meijer, E. W. *Macromolecules* **2005**, *38*, 3176–3184.
(9) Meyer, W. C.; Woo, J. T. K. *J. Phys. Chem.* **1969**, *73*, 3485–3488.
(10) Jadýn, J.; Stockhausen, M.; Žywucki, B. *J. Phys. Chem.* **1987**, *91*, 754–757.
(11) Lehn, J.-M. *Science* **1993**, *260*, 1762–1763.
(12) Lehn, J.-M. *Supramolecular Chemistry*; VCH: Weinheim, 1995.
(13) Sijbesma, R. P.; Beijer, F. H.; Brunsveld, L.; Folmer, B. J. B.; Hirschberg, J.; Lange, R. F. M.; Lowe, J. K. L.; Meijer, E. W. *Science* **1997**, *278*, 1601–1604.
(14) Folmer, B. J. B.; Sijbesma, R. P.; Versteegen, R. M.; Rijt, J. A. J. v. d.; Meijer, E. W. *Adv. Mater.* **2000**, *12*, 874–878.
(15) Söntjens, S. H. M.; Sijbesma, R. P.; Genderen, M. H. P. v.; Meijer, E. W. *J. Am. Chem. Soc.* **2000**, *122*, 7487–7493.
(16) van Beek, D. J. M.; Gillisen, M. A. J.; van As, B. A. C.; Palmans, A. R. A.; Sijbesma, R. P. *Macromolecules* **2007**, *40*, 6340–6348.
(17) Yamauchi, K.; Kanomata, A.; Inouie, T.; Long, T. E. *Macromolecules* **2007**, *37*, 3519–3522.
(18) Lange, R. F. M.; Gurp, M. v.; Meijer, E. W. *J. Polym. Sci., Part A* **1999**, 3657–3670.
(19) Yamauchi, K.; Lizotte, J. R.; Long, T. E. *Macromolecules* **2003**, *36*, 1083–1088.
(20) Elkins, C. L.; Park, T.; McKee, M. G.; Long, T. E. *J. Polym. Sci., Part A* **2005**, *43*, 4618–4631.
(21) McKee, M. G.; Elkins, C. L.; Park, T.; Long, T. E. *Macromolecules* **2005**, *36*, 6015–6023.
(22) Janssen, H. M.; van Gemert, G. M. L.; ten Cate, A. T.; van Beek, D. J. M.; Sijbesma, R. P.; Meijer, E. W.; Bosman, A. W. WIPO Suprapolix B.V. WO, 2004/016598.
(23) van Gemert, G. M. L.; Versteegen, R. M.; Janssen, H. M.; Meijer, E. W.; Bosman, A. W. WIPO Suprapolix B.V. WO 2006/006844 A1.
(24) Dankers, P. Y. W.; van Leeuwen, E. N. M.; van Gemert, G. M. L.; Spiering, A. J. H.; Harmsen, M. C.; Brouwer, L. A.; Janssen, H. M.; Bosman, A. W.; van Luyn, M. J. A.; Meijer, E. W. *Biomaterials* **2006**, *27*, 5490–5501.
(25) Ono, H.-K.; Jones, F. N.; Pappas, S. P. *J. Polym. Sci., Polym. Lett.* **1985**, *23*, 509–515.
(26) Fraga, I.; Montserrat, S.; Hutchinson, J. M. *J. Therm. Anal. Calorim.* **2007**, *87*, 119–124.
(27) Höper, R.; Gesang, T.; Possart, W.; Hennemann, O.-D.; Boseck, S. *Ultramicroscopy* **1995**, *60*, 17–24.
(28) Kautz, H.; van Beek, D. J. M.; Sijbesma, R. P.; Meijer, E. W. *Macromolecules* **2006**, *7*, 919–926.
(29) Dankers, P. Y. W.; Harmsen, M. C.; Brouwer, L. A.; van Luyn, M. J. A.; Meijer, E. W. *Nat. Mater.* **2005**, *4*, 568–574.
(30) Krenning, G.; Dankers, P. Y. W.; Jovanovic, D.; van Luyn, M. J. A.; Harmsen, M. C. *Biomaterials* **2007**, *28*, 1470–1479.
(31) Dankers, P. Y. W.; van Gemert, G. M. L.; Janssen, H. M.; Meijer, E. W.; Bosman, A. W. WIPO Suprapolix B.V. WO 2006/118461.

MA800744C